D 11.8: Simulation results for a calorimeter

The present report summarizes the work on simulations for the response of calorimetric (with spectroscopic capabilities) detectors, presenting a realistic simulation of a high granularity and resolution calorimeter, made of CsI[Tl] crystals. The techniques herein discussed and implemented in the simulation and data analysis framework developed for SiNuRSE, EnsarRoot, will serve to improve the exploitation of the existing facilities and the accuracy of the experiments through the optimisation of their calorimetric detection systems and to benefit future activities and developments in the field.

The response of a scintillator detector can be modeled in EnsarRoot following any of the included examples: simple scintillator models for different applications (modules scintillator_template and scitof) or a complete calorimeter/spectrometer simulation, with different analysis macros. The EnsarRoot documentation describes the classes in each example and shows how to modify them to describe advanced setup.

Performance analysis tools for calorimetry

Several tools have been developed in order to evaluate the performance of calorimeter detectors. These tools include event generators, geometrical description templates, simple reconstruction models (hit finder) and visualization and reporting macros for the analysis.

The evaluation of the performance of calorimeter detectors under different physics scenarios requires the construction of appropriate event generators. Several event generators have been developed, ranging from trivial gamma ray and particle distributions for testing the characteristics of the detector, to complex experimental multi-particle decay events, to evaluate the reconstruction capabilities. A flexible code producing distributions of gamma rays or charged particles is integrated within the EnsarRoot event generators. The generator allows the selection of the particle type, angular emission (both in polar and azimuthal angles or any angular region), the momentum (or momentum range), multiplicity and position of the emitted particles. Additional functions allow the generation of a flat distribution on the cosine of the polar angle for an isotropic angular emission, the random location of the vertex inside a volume which simulates an interaction within the target and the addition of the Lorentz boost for gamma rays, with selectable projectile velocity.

For nuclear spectroscopy and the study of Giant and Pygmy resonances, a gamma ray cascade generator has been included (CascadeGen[1]). The input for the generator is an

[1] Courtesy Enrique Nacher (CSIC-IEM), with permission.

ASCII text file in which the user can set the speed of the projectile (β, for generating the Lorentz boost), its uncertainty due to the thickness of the target, and the main characteristics of the de-excitation pattern. The latter includes the position of a Giant Dipole Resonance (GDR), a Pygmy Dipole Resonance (PDR) if applicable, their respective widths, the probability to populate each of the resonances in the reaction, the position of all the spectroscopic levels, the probability to populate each level in the reaction, and finally, a branching ratio matrix which connects all the different levels and the resonances. The gamma ray cascade generator can be used to generate events with low multiplicity and low energy gamma rays instead of GDR examples, simply by setting the probability to populate the resonance equal to zero and defining a simple level scheme containing a few low-energy levels.

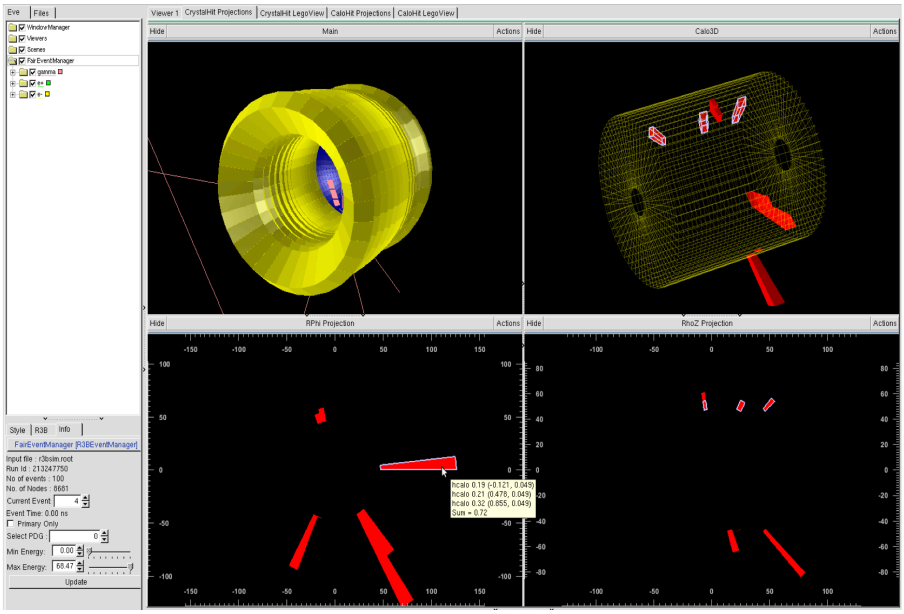

Fig. 1: Event display showing the simulated tracks, a perspective view of the calorimeter and longitudinal and transversal cuts of the energy deposited in the calorimeter crystals. The length of the bars is proportional to the energy deposited in each crystal.

An "ascii" file input option allows the input from an event list-mode file, where events are individually listed by multiplicity, identifying the participant particle identifiers (particle ID or atomic number, mass and charge state for ions) their momenta and starting position. In this way, other event generators not coupled with EnsarRoot can be easily interfaced. Regarding geometry description: For complex geometries, the ROOT TGeo description should be removed from the code and added as a external ROOT file, which could be loaded in execution time. This procedure saves time and memory and allows for a modular setup description. An example is given in the module calo. For simpler geometries, models of implementation are given in the templates directories.

For the reconstruction and the analysis, tasks and macros have been included within the calo module covering simple particle reconstruction by add-back methods. A

geometrical search on close crystals (for instance within a cone or a square window around the crystal with the largest energy deposition) allows add-back on small portions of the calorimeter for the reconstruction of events with multiplicity larger than one. Analysis and report macros are also included (calo/macros in EnsarRoot) and can be taken as examples for further development.

Finally, a visualization set of macros runs the event display manager for simulation events, shown in Fig. 1. The event display selects different views (in the figure, 3D views for the simulated tracks and the crystal hits and longitudinal and transversal views for the crystal hits) for the information in the crystals or in the clusters obtained from the hit finder methods.

Results for a complex calorimeter simulation

The response of a calorimeter is exemplified within the EnsarRoot framework with the simulation and analysis code for the CALIFA calorimeter. A complete report describing the outcome of the simulation for the entire CALIFA Barrel section has been published (H. Alvarez-Pol *et al.*, "Performance analysis for the CALIFA Barrel calorimeter of the R3B experiment". Nuclear Instruments and Methods in Physics Research Section A 767 (2014) 453-466).

CALIFA is an advanced detector for gamma rays and light charged particles, accordingly optimized for the demanding requirements of the physics programme proposed for the R^3B facility at FAIR: a good energy resolution (5-6% at 1 MeV for gamma rays) and high efficiency, for gamma rays emitted from fast projectiles (around 700 A MeV). Charged particles, e.g. protons of intermediate energies (up to 320 MeV in the Barrel section of CALIFA, covering between 43.2º and 140.3º, should be also identified with an energy resolution better to 1%. CALIFA is divided in two well-separated sections, a ``Forward EndCap" and a cylindrical ``Barrel" covering an angular range from 43.2 to 140.3 degrees. The Barrel section, based on long CsI(Tl) pyramidal frustum crystals coupled to large area avalanche photodiodes (LAAPDs), attains the requested high efficiency for calorimetric purposes.

The assessment of the capabilities and expected performance of the detector elements is a crucial step in their design, along with the prototypes evaluation. For this purpose, the Barrel geometry has been carefully implemented in the simulation package EnsarRoot (from the original R3BRoot code), including easily variable thicknesses of crystal wrapping and carbon fibre supports. A complete characterization of the calorimeter response (including efficiency, resolution, evaluation of energy and reconstruction losses) under different working conditions, with several physics cases selected to probe the detector performance over a wide range of applications, has been undertaken.

The CALIFA Barrel and the complete calorimeter have been tested using gamma rays emitted with energies between 200 keV and 15 MeV in the projectile frame (β=0.82). The crystal intrinsic non-uniformity has been included by simulating a 1% maximum

random deviation from the original energy deposited in the scintillator material. A Gaussian smearing of 4%, 5% and 6% at the energy of 1 MeV, scaling with the square root of the energy, has been used to represent the experimental resolution. "Perfect" detectors, with no energy smearing, have been additionally simulated to represent the geometrical contribution to the total resolution.

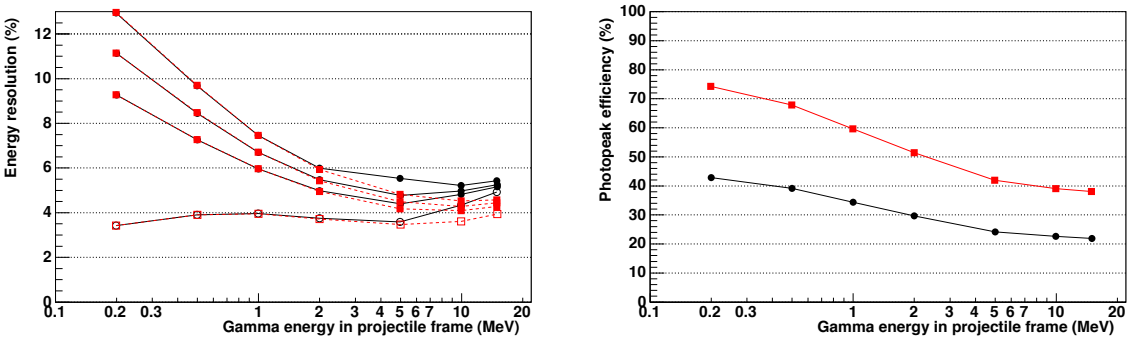

Fig. 2: [Left pad]: Dependence of the resolution with the emitted gamma ray energy in projectile frame. From the top to the bottom, in solid circles and lines, results for intrinsic resolution of 6%, 5% and 4% at 1 MeV (scaling with the square root of the energy) are displayed. The lower curve (open markers) corresponds to ideal detectors. The squares represent the same set of curves with add-back in all the calorimeter crystals. [Right pad]: dependence of the photopeak efficiency with the emitted projectile-frame gamma-ray energy for the Barrel. The square markers represent the photopeak efficiency normalized to the number of gamma rays emitted in the CALIFA Barrel geometrical acceptance, while the circles correspond to the total emitted gamma rays, independent of their direction.

The energy resolution is defined as $R=FWHM/E\gamma \approx 2.355\ \sigma/E\gamma$, where σ and $E\gamma$ are obtained from the Gaussian fit to the photopeak. The left pad of Fig. 2 shows the dependence of the resolution with the emitted gamma ray energy in the projectile frame for the full calorimeter. The different curves (solid lines and circles) correspond to different values of the crystals energy resolution: from the top to the bottom results for an experimental intrinsic resolution of 6%, 5% and 4% at 1 MeV (scaling with the square root of the energy) are displayed, while the lower curve (open markers) corresponds to ideal detectors, where the sole contribution to the resolution is the Lorentz broadening. The additional set of square markers (dashed lines) represents the case where a sum over all crystals was employed. They differ only at high energy, 5 MeV and above, where the resolution is better when all the crystals energies are added. This difference is an indication that, for the most energetic gamma rays, part of the energy could escape to large distances from the initial interaction point, complicating the reconstruction of clusters. Selecting a larger angular window would include this portion of the energy, conversely decreasing the efficiency for events with larger multiplicity. At low energies, the energy resolution is dominated by the intrinsic crystal resolution. At larger energies, above 2 MeV in the projectile frame, the granularity of the detector dominates, with the Lorentz broadening becoming the larger contribution to the energy resolution as the energy increases. It is worth noting that the granularity has been chosen to reduce the geometrical contribution to the energy resolution to approximately 4%.

The efficiency of the CALIFA Barrel has been one of its key requirements and a huge effort has been dedicated to improve this feature in the calorimeter concept and design. The photopeak or full absorption efficiency is the key parameter in this evaluation. It is defined as the ratio between the number of gamma rays which are reconstructed with their complete energy and the total number of emitted gamma rays. The definition depends on what "complete energy reconstruction" is considered. Here, the energies included within a window in the interval [-2σ, 2σ] of the Gaussian function fit of the photopeak have been taken. This criterion is quite conservative at low energies, discarding entries in the tails of the peak which could be considered as well reconstructed. But it is useful to avoid the inclusion of reconstructed gamma energies in the left part of the photopeak for the largest energies, where the photopeak shape deviates from a Gaussian distribution.

The right pad of Fig. 2 represents the photopeak efficiency. Here, both the geometrical acceptance uncorrected (circle markers) and corrected (square markers) photopeak efficiencies are shown; the first curve indicates the efficiency combining intrinsic and acceptance effects, while the second is corrected by the geometrical acceptance of the Barrel. In both cases the algorithm uses an optimized angular window to cope with multiplicities larger than one.

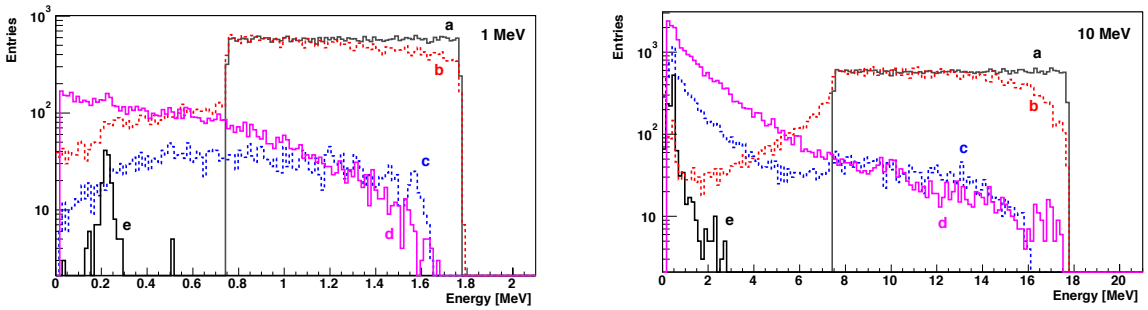

Fig. 3: [Left pad]: energy spectra in the different regions and escaping zones for emitted gamma rays of 1 MeV in projectile frame. The line labeled a corresponds to the emitted energy spectrum, line b is the sum energy spectrum in the crystals and below, lines c and e correspond to the energy which escape beyond the Barrel outer surface and through the backward angle aperture, respectively. Line d corresponds to the energy spectrum absorbed by the passive matter. [Right pad]: energy spectra in the different regions and escaping zones for emitted gamma rays of 10 MeV in projectile frame. Labels are equivalent to those of the left pad.

The evaluation of where the undetected energy has been stopped is very important to improve the calorimeter design. Part of the Compton scattered or the backscattering gamma rays could escape the detector through the backward angles aperture, not covered by crystals. Another part, mainly at the highest energies, could escape after passing through the detector Barrel crystals. To perform a realistic evaluation, the simulation considers gamma rays emitted at different energies in the projectile frame and, therefore, the energies at the Barrel vary with the polar angle. The angular range of the emitted particles has been constrained to the geometrical aperture of the Barrel section.

Fig. 3 shows the energy spectra emitted and absorbed in the calorimeter elements, when gamma rays of 1 MeV (left pad) and 10 MeV (right pad) in the projectile frame are emitted, again boosted at a velocity β=0.82. The energy spectra correspond to detection of gamma rays at laboratory energies and, therefore, the spectra are influenced by the kinematics of the Lorentz boost; this result is evident in the emitted gamma rays spectrum (line a), with a flat energy distribution ranging from around 0.7 to 1.8 times the projectile frame energy. Immediately below, the next histogram (line b) corresponds to the energy spectrum in the crystals, that is, the detected energy. Below, in lines c and e, the energy which escapes beyond the Barrel outer surface and through backward angle aperture are displayed, respectively. The last histogram, line d, corresponds to the energy spectrum which is not detected in any of the previous elements, that is, the energy absorbed by the inactive matter between the emission point and the end of the gamma ray life.

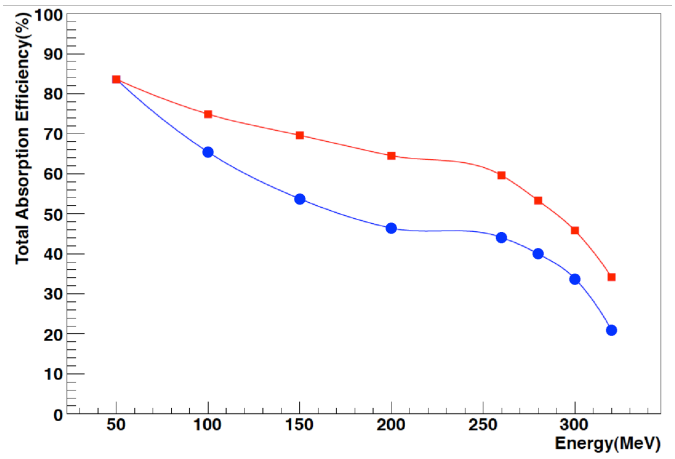

Fig. 4: Total absorption efficiency for mono-energetic protons emitted within the angular coverage of the CALIFA Barrel, obtained by integrating the area below the peak (two sigma criteria, lower curve, circles) or by integrating the area below the peak from 90% of the nominal energy (upper curve, squares).

We have also calculated the total absorption efficiency of the CALIFA Barrel for mono-energetic protons emitted within the angular coverage of the Barrel. In fact, for the highest energies, we have focused on the furthest forward angles as they are of particular importance for the planned study of (p,2p) reactions. Due to the particular kinematics of these reactions, in most of the cases we will have one proton in the direction of the forward EndCap and the other (with expected energies up to 320 MeV) directed towards the furthest forward rings of the Barrel.
With the aim of testing the performance of the Barrel in this situation, we have generated mono-energetic protons of energies between 50 MeV and 200 MeV emitted isotropically within the angular acceptance of the Barrel, and mono-energetic protons of energies between 260 MeV and 320 MeV emitted in the most forward angles covered by the Barrel. The energy deposited in the crystals has been collected and summed. The intrinsic scintillator energy resolution has been adjusted to 5% at 1 MeV.

Fig. 4 shows the total absorption efficiency of the Barrel for protons as a function of the energy. The two different curves correspond to the efficiency obtained according to two different criteria. The lower curve (circles) represents the efficiency calculated by integrating the area below the total absorption peak within a window in the interval [-2σ, 2σ]. The upper curve (squares) represents the efficiency calculated by integrating the peak from the point at 90% of the nominal energy. The former definition applies more to spectroscopic applications in which the energy resolution is the most important parameter, whereas the latter applies more to calorimetric purposes in which the efficiency is the most important parameter and we just need to be sure that we have measured at least 90% of the energy of the incoming proton. In fact, an optimization of the algorithm correcting the proton energy according to the multiplicity would increase the efficiency defined by the former definition, leading to very similar results.

This evaluation of the performance of a complex calorimeter allows the assessment of its main features, including its energy resolution, efficiency, passive vs. active matter balance and high-multiplicity reconstruction capabilities. These characteristics can be evaluated systematically over a broad energy and angular emission range, for the species that the calorimeter is sensitive to, namely gamma rays and charged particles, and also for key physical cases of interest, provided by the wide possible interface of the event generators accepted in EnsarRoot. The evaluation constitutes an accurate estimate of the final capabilities of the calorimeter before its construction and justifies the selected design, confirming that it achieves the required capabilities. It also aids in the design of ancillary and complementary detectors for the setup.